

Lattice position of Hf and Ta in LiNbO_3 : An extended x-ray-absorption fine-structure study

C. Prieto

*Instituto de Ciencia de Materiales de Madrid, Consejo Superior de Investigaciones Científicas,
Campus Universitario de Cantoblanco (C-IV), 28049 Madrid, Spain
and Laboratoire pour l'Utilisation du Rayonnement Electromagnétique, Université de Paris-Sud
(Bâtiment 209D), 91405 Orsay, France*

C. Zaldo

*Instituto de Ciencia de Materiales de Madrid, Consejo Superior de Investigaciones Científicas,
Campus Universitario de Cantoblanco (C-IV), 28049 Madrid, Spain*

P. Fessler and H. Dexpert

*Laboratoire pour l'Utilisation du Rayonnement Electromagnétique, Université de Paris-Sud
(Bâtiment 209D), 91405 Orsay, France*

J. A. Sanz-García and E. Diéguez

Departamento de Física Aplicada (C-IV), Universidad Autónoma de Madrid, 28049 Madrid, Spain

(Received 7 June 1990)

The lattice position of Hf and Ta impurities in LiNbO_3 single crystals has been investigated using fluorescence extended x-ray-absorption fine-structure (EXAFS) spectroscopy. It has been concluded that Hf is in the lithium octahedron and Ta ions are in the niobium one. Both impurities lie very close to the center of the oxygen octahedron.

I. INTRODUCTION

LiNbO_3 is a relevant material because of its application to optoelectronics technology as optical waveguide,¹ photorefractive devices,² and solid-state matrix.³

In all those applications the foreign ions in the material play a major role because they are responsible for the modification of the optical properties of the matrix: (a) Optical waveguides are commonly created in LiNbO_3 by diffusing Ti at high temperature.¹ The Ti ions change the refractive index of the substrate. In some cases Mg-doped substrates are used in order to enhance the optical damage threshold.⁴ (b) Photorefractive properties are introduced by doping the crystal with transition-metal ions (mainly iron);² these impurities introduce electronic levels which act as photoexcitable donors or traps. (c) Rare-earth ions (Nd and others) have been studied as possible impurities to produce solid-state lasers.¹³

In order to fully understand the optical modifications introduced by the impurities, their lattice location should be elucidated. Previous electron paramagnetic resonance (EPR) and Mössbauer spectroscopy experiments have indicated that the lattice location of transition-metal and rare-earth ions shows trigonal symmetry.⁵ Nb and Li substitutional sites are possible, whereas the intrinsic vacancy one is not generally considered. So far, no conclusive evidence favoring a particular site has been obtained for most impurities, except for a few cases: Extended x-ray-absorption fine-structure (EXAFS) spectroscopy has revealed that Mn is in the Li site in a centered position.⁶ This is in agreement with the conclusions of

previous EPR and electron-nuclear double resonance (ENDOR) works.^{7,8} Rutherford-backscattering (RBS) channeling experiments have been also applied recently to determine the lattice position of impurities in LiNbO_3 . It has been concluded that Eu lies in both Li and Nb sites⁹ with occupancy factors of 36% and 64%, respectively, and that Hf and Nd are sited in the Li octahedron,^{10,11} the vacancy site being free of impurities.

In this work we intend to resolve the lattice location of Hf and Ta impurities in LiNbO_3 by using EXAFS spectroscopy. These results are expected to be a valuable reference for the previous conclusions obtained by RBS experiments in the case of Hf and to be a model for future work in the case of Ta, since one would expect that Ta is in the Nb site because of the isomorphism between LiNbO_3 and LiTaO_3 .

EXAFS fluorescence technique is required to deal with the low concentration of impurity in the samples used for optical applications. The relative large atomic number of Nb is also an added difficulty for absorption measurements. The fluorescence spectra we have obtained are rather noisy due to the low impurity concentration. Additionally, the analysis of the fluorescence spectra is less accurate than for absorption because of the autoabsorption of the fluorescence in the sample. Those facts limit the accuracy of the determination of the atomic distances and coordination numbers. However, the analysis of the spectra can provide unambiguous evidence to select a definite lattice site.

The results presented in this work show that Hf is in the Li octahedron and Ta in the Nb one.

II. EXPERIMENTAL TECHNIQUES

Stoichiometric LiNbO₃ single crystals have been grown in the Crystal Growth Laboratory of Universidad Autónoma of Madrid by the Czochralski method. 1% of HfO₂ and Ta₂O₅ were added to the melt. The Hf and Ta molar concentration in these crystals has been estimated from RBS experiments as 1.3% and 1%, respectively.

The expected valence of the ions incorporated to the lattice are Hf⁴⁺ and Ta⁵⁺. This expectation has been experimentally confirmed by us from the comparison of the x-ray absorption near-edge structure (XANES) *L*_{III} spectra of Hf and Ta in LiNbO₃ with those of HfO₂ and LiTaO₃, respectively.

The samples were plates cut with their large faces perpendicular to the *c* axis. This axis was placed in the horizontal plane of the machine and tilted about 45° with regard to the x-ray beam. Bragg diffractions were avoided by spatially shielding the detector window.

Fluorescence spectra were acquired at room temperature (RT) at the *L*_{III} edges of Hf (9561 eV) and Ta (9881 eV). We used synchrotron radiation emitted by the L.U.R.E. (Orsay) D.C.I. storage ring, running at 1.85 GeV, at the EXAFS-IV beam station, with an average current of 250 mA. X-rays were monochromatized using a Si(311) two-crystal spectrometer.

Detection of the fluorescence has been made by a multiwire proportional counter.^{12,13} The detector, swept with an Ar-CO₂ (90-10 %) mixture at 200 nPa above atmospheric pressure, was directly fixed on the sample chamber. The solid angle of detection was estimated to be 0.32π st.

Data were recorded under good linearity and efficiency conditions due to the presence of a drift and delay line (300 ns) on each cathode plane.¹⁴

III. EXPERIMENTAL RESULTS AND DATA ANALYSIS

A. Hf-doped samples

Figure 1(a) shows the x-ray fluorescence spectrum $\mu(E)$ of the Hf-doped LiNbO₃. A classical procedure has been used to analyze the EXAFS spectrum: Above the edge, the signal background is removed by a multi-iteration curve-smoothing procedure. The EXAFS signal $\chi(E)$ obtained is shown in Fig. 1(b) (dots).

The analysis of the EXAFS signal to get the position of the neighbors around the impurity has been carried out using the well-known EXAFS expression¹⁵

$$\chi(k) = \sum_j \frac{N_j}{kR_j^2} \exp(-2k^2\sigma_j^2) \exp\left[\frac{-\Gamma_j R_j}{k}\right] f_j(k) \times \sin[2kR_j + \phi_j(k)]. \quad (1)$$

This expression describes the EXAFS oscillations for a Gaussian distribution of neighbors around the central atom, in the single scattering theory and in the plane-wave approximation. k is the wave vector of the photoelectron, which is related to the electron mass (m_e) and with the threshold energy (E_0) by

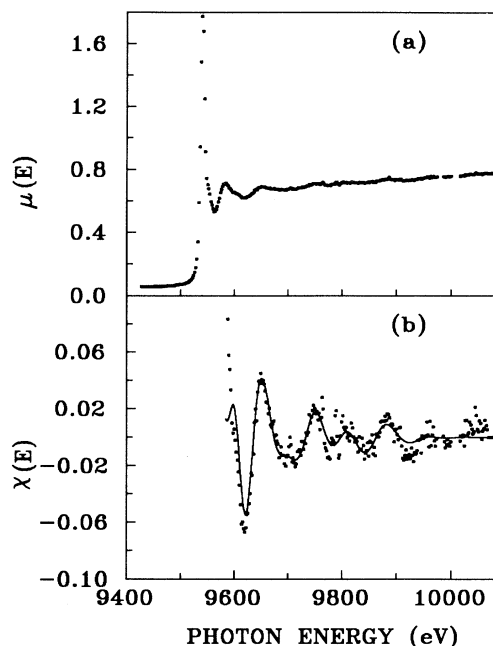


FIG. 1. (a) Room-temperature x-ray fluorescence yield $\mu(E)$ of LiNbO₃ doped with 1% of Hf measured at the *L*_{III} edge of Hf. (b) EXAFS signal $\chi(E)$ extracted from the experimental fluorescence spectrum (dots). EXAFS signal reproduced by the three significant peaks of the pRDF function of Fig. 2(a) obtained by back-Fourier transform in the range 1.3–3.9 Å (solid line).

$$k = \left[\frac{2m_e}{\hbar^2} (E - E_0) \right]^{1/2}. \quad (2)$$

N_j is the average coordination number for the Gaussian distribution of distances centered at the R_j value, σ_j is the Debye-Waller contribution, $\phi_j = 2d + Y_j(k)$ is the phase shift, d and Y_j being the central and backscattering atom phase shifts, respectively, $f_j(k)$ is the amplitude of the backscattering atoms, and Γ_j is related to the mean free path of the photoelectron.

Figure 2(a) shows the Fourier transform of the $k^3\chi(k)$ weighted signal (hereafter we refer to this function as pRDF). The peaks which appear in this function have to be corrected by the $\phi_j(k)$ contribution to obtain the “true” distances of the defect.

Figure 2(a) shows three main peaks at 1.65, 2.4, and 3.0 Å (denoted as I, II, and III, respectively) which are to be related to the oxygen and niobium neighbors. The presence of those peaks has been found to be essentially independent of the Fourier transform procedure, and most of the information on the EXAFS spectrum is included in them since the back-Fourier transform of the pRDF function is the limited range 1.3–3.9 Å approximately reproduces the EXAFS oscillations [see Fig. 1(b), solid line].

In order to get a qualitative knowledge of the ligands responsible for the peaks observed in Fig. 2(a), we have calculated the backscattering amplitude $f_j(k)$ of peaks I

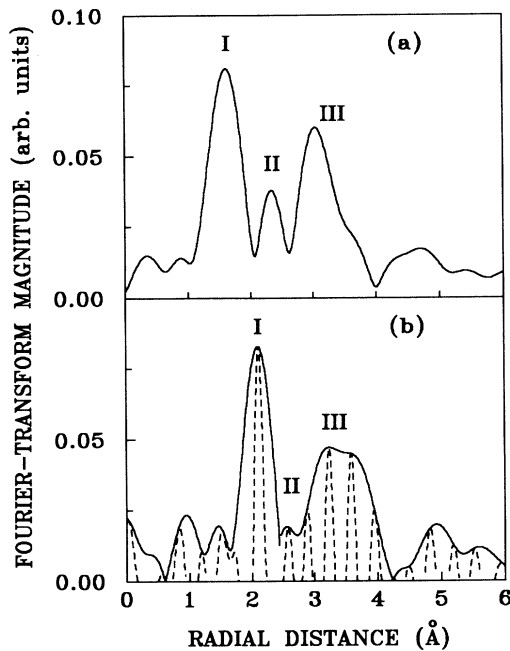


FIG. 2. (a) Fourier transform (pRDF) of the $k^3\chi(k)$ weighted EXAFS signal of Hf-doped LiNbO_3 . A Hanning window over 500 eV was used for apodization. (b) Radial distribution function (RDF) calculated as the modulus of the expression (3) by using theoretical amplitude and phase functions according to the expected backscattering atoms (solid line). Positive values of the imaginary part of the same expression (dashed line). The left part of the plot until 2.2 Å has been calculated assuming Hf-O pairs and the right part for the Hf-Nb pairs.

and III of Fig. 2(a). To perform these calculations the selected peaks were filtered individually, and assumed realistic values were used for N_j and R_j ; also $\sigma_j=0$ and $\Gamma_j=0$ were assumed. No similar procedure was used for peak II of Fig. 2(a) because of the overlapping with the side peaks.

Figure 3(a) shows the backscattering amplitudes obtained. The plot shows that peak I of Fig. 2(a) corresponds to a light element such as oxygen. On the other hand, the dependence of peak III looks similar to that expected for niobium.

To determine further the nature of the ligands responsible for peaks I, II, and III of Fig. 2(a), we have used the method proposed by Lee and Beni.¹⁶ Following this method, we have calculated for each peak the function $\rho_j(r')$ defined as

$$\rho_j(r') = \int_{k_1}^{k_2} \left[\frac{k^n \chi(k)}{f_j(k)} e^{-i\phi_j(k)} e^{-2\sigma_j^2 k^2} \right] e^{i2kr'} dk, \quad (3)$$

and varied the energy threshold until the matching of the peaks (within the same shell) of the imaginary part and the modulus of the $\rho_j(r')$ is obtained. To perform the calculation we have used the theoretical phase and amplitude functions reported by McKale *et al.*¹⁷ and assumed $\Gamma_j=0$ and $\sigma_j=0$.

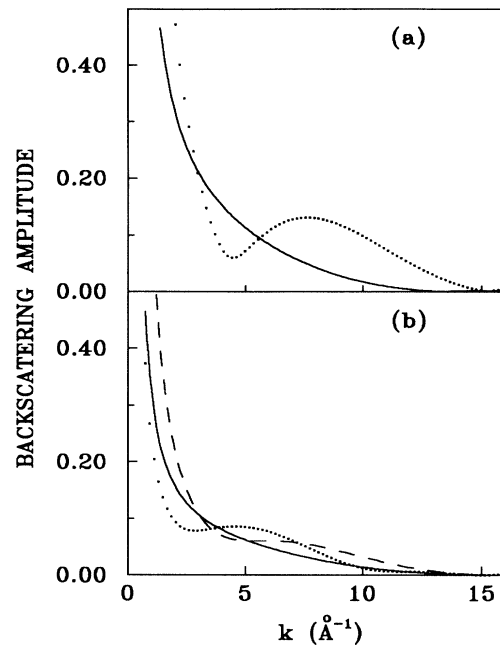


FIG. 3. Backscattering amplitudes of the pRDF peaks of doped LiNbO_3 calculated for the N_j and R_j values reported in the brackets. (a) Hf-doped LiNbO_3 : 1.6-Å peak ($N_j=6$ and $R_j=2.0$ Å) (solid line); 3.0-Å peak ($N_j=3$ and $R_j=3.3$ Å) (dotted line). (b) Ta-doped LiNbO_3 : 1.56-Å peak ($N_j=6$ and $R_j=2.0$ Å) (solid line); 3.46-Å peak ($N_j=6$ and $R_j=3.7$ Å) (dashed line); 5.08-Å peak ($N_j=12$ and $R_j=5.3$ Å) (dotted line).

Figure 2(b) shows the real and imaginary part of $\rho(r')$ obtained under the assumption that peak I is due to oxygen and peaks II and III to niobium. The good matching obtained confirms the assignments obtained from Fig. 3(a) for peaks I and II and additionally suggests that peak II is due to the presence of niobium ions.

To obtain a more accurate determination of the crystallographic distances, we have minimized (using a standard minimization procedure) the difference between the experimental filtered data and the function $\chi(k)$ calculated according to Eq. (1) using the corresponding amplitudes and phases reported by McKale *et al.*¹⁷ In the refinements the coordination number has been chosen according to the oxygen and niobium spheres expected for the Li octahedron (see Sec. IV). Figure 4 shows the comparison in distance space of the experimental data and the calculated radial distribution function. The best fit is obtained for the R_j , σ_j , Γ_j and ΔE_0 set of values summarized in Table I.

The Debye-Waller factor obtained from the fitting of the Hf spectrum (and also for Ta one presented later) can be compared with those reported for stoichiometric LiNbO_3 from x-ray-diffraction experiments.¹⁸ The values obtained for the best fit are close to the thermal displacements reported for niobium (0.06) and for oxygen atoms (0.08) of the lattice.

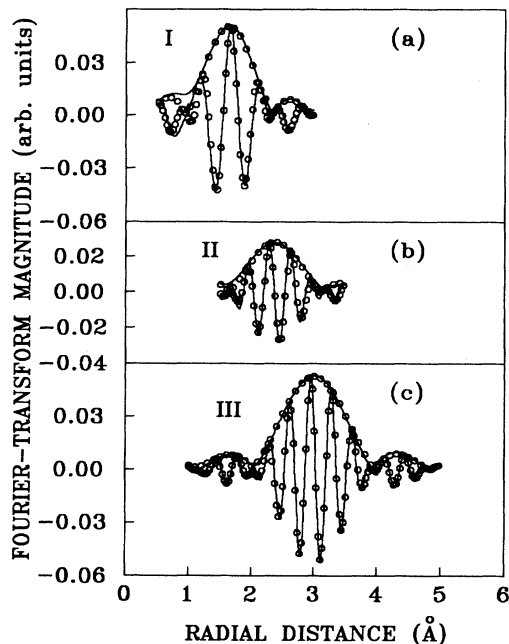


FIG. 4. LiNbO₃:Hf. Distance space comparison between calculated pRDF (solid line) and experimental filtered data (discrete points) of the modulus and imaginary part of the Fourier transform for the three peaks appearing in Fig. 2(a).

B. Ta-doped samples

Figure 5(a) shows the x-ray fluorescence spectrum of Ta-doped LiNbO₃. Figure 5(b) shows the EXAFS signal obtained from Fig. 5(a), which appears attenuated as compared with the Hf case.

The Fourier transform of the EXAFS signal is shown in Fig. 6(a) (continuous line). Three well-resolved peaks appear at 1.56, 3.46, and 5.08 Å; those peaks have been denoted as I, III, and IV, respectively.

Figure 3(b) shows the backscattering amplitudes corresponding to peaks I, III, and IV of Fig. 6(a). The behavior of the $f_j(k)$ function corresponding to the peak I looks like that expected for oxygen as a backscatterer, whereas those of the peaks III and IV look like that ex-

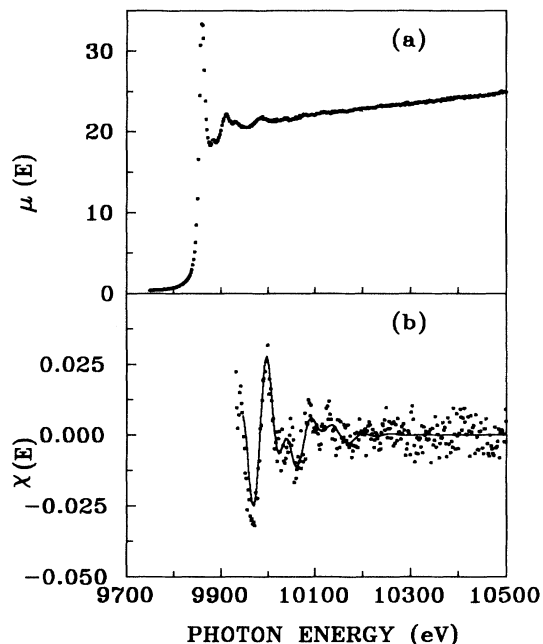


FIG. 5. (a) Room-temperature fluorescence yield $\mu(E)$ of LiNbO₃ doped with 1% of Ta, measured at the L_{III} edge of Ta. (b) EXAFS signal $\chi(E)$ extracted from the experimental fluorescence spectrum (dots). EXAFS signal reproduced by the significant peaks of the pRDF function of (a) obtained by back-Fourier transform of the 1.3–4.1-Å range (solid line).

pected for niobium.

Additionally, in Fig. 6(a) a minor peak (denoted as II) is observed at 2.56 Å. The calculation of the amplitude of this peak is not reliable because of the overlap with the side peaks. To get a better understanding of its origin, as well as to confirm the assignments made before, we have again used the Lee-Beni method described in Sec. III A.

Figure 6(b) shows the matching between the modulus and imaginary part of the $\rho(r')$ function for each peak of Fig. 6(a). The agreement is obtained for peak I when the oxygen phase and amplitude are selected, and for peaks III and IV when the niobium phase and amplitude are used. However, no matching is obtained for peak II, as-

TABLE I. Summary of the values of R_j , σ_j , Γ_j , and ΔE_0 obtained.

Compound	Pair	N_j	R_j (Å)	σ_j (Å)	Γ_j (Å ⁻²)	ΔE_0 (eV)
Hf:LiNbO ₃	Hf-O	6	2.07	0.094	2.2	12
	Hf-Nb	1	2.57	0.089	2.2	25
	Hf-Nb	6	3.30	0.085	2.2	30
Ta:LiNbO ₃	Ta-O	6	1.96	0.115	4.1	10
	Ta-Nb	6	3.68	0.101	4.1	18
	Ta-Nb	12	5.26	0.090	4.1	10
LiTaO ₃	Ta-O	6	1.99	0.112	4.1	3
	Ta-Ta	6	3.41	0.106	4.1	10

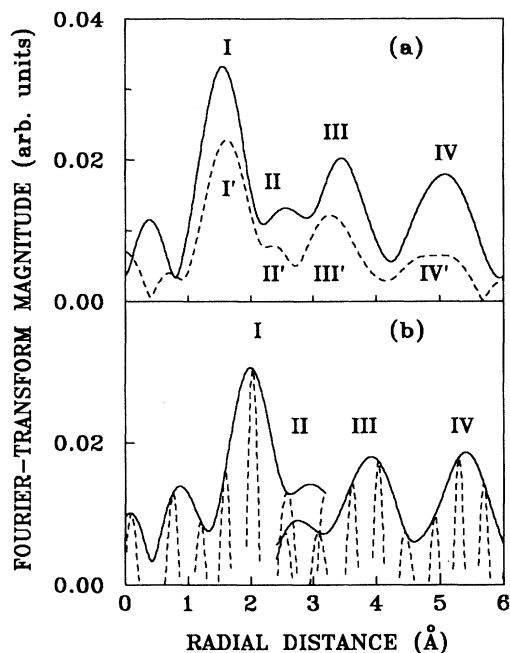


FIG. 6. (a) Fourier transform (pRDF) of the $k^3\chi(k)$ weighted EXAFS signal of Ta-doped LiNbO_3 (solid line). A Hanning window over 500 eV was used for apodization. The dashed line gives the same function for the LiTaO_3 under the same conditions. (b) The radial distribution function (RDF) for the Ta-doped sample calculated as the modulus of the expression (3) by using the theoretical amplitude and phase functions of Mckale *et al.* according to the expected backscattering atoms (solid line). Imaginary part of the same expression (dashed line). The left part of the plot until 2.2 Å has been calculated assuming Ta-O pairs and the right part for the Ta-Nb pairs.

suming either oxygen or niobium neighbors.

As discussed in Sec. III A, to obtain more accurate crystallographic distances we have minimized the difference between the experimental and calculated data for $\chi(k)$. Figure 7 shows the best fit obtained for the significant peaks shown in Fig. 6(a). The R_j , σ_j , Γ_j and ΔE_0 set of values obtained for the best fit are also summarized in Table I.

Additionally, we have compared the fluorescence EXAFS spectra of Ta, in LiNbO_3 with that of a LiTaO_3 single crystal. The pRDF function of LiTaO_3 calculated under identical conditions to those used in the data treatment of Ta-doped LiNbO_3 is included in Fig. 6(a) (dashed line). It is worth noting the similarity between the spectra.

In LiTaO_3 there are two different, rather close, Ta-O distances which do not appear to be resolved in Fig. 6(a). These distances have been calculated by x-ray diffraction¹⁹ as 1.89 and 2.07 Å and by neutron diffraction²⁰ as 1.91 and 2.07 Å. The EXAFS results under the present experimental and analytical conditions give a distance for the Ta-O pairs of 1.99 Å, which is in fairly good agreement with the average of the distances for the six oxygen pairs reported by neutron diffraction.

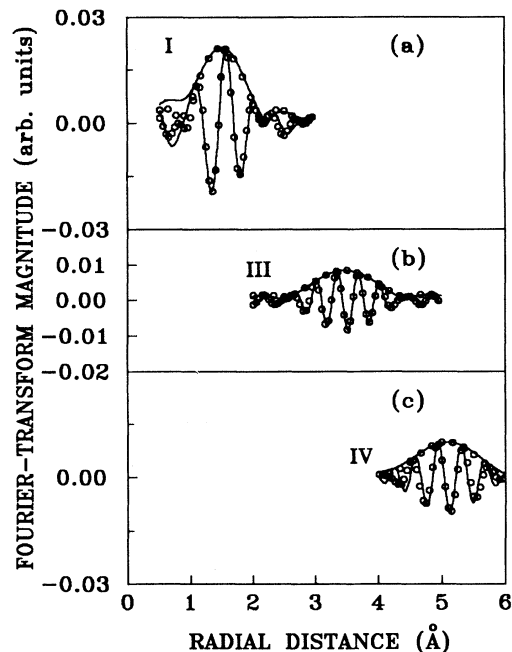


FIG. 7. $\text{LiNbO}_3:\text{Ta}$. Distance space comparison between the calculated pRDF (solid line) and experimental filtered data (discrete points) of the modulus and imaginary part of the Fourier transform for the three peaks appearing in Fig. 5(a).

Thus, within an uncertainty of about 0.15 Å, the use of the theoretical amplitude and phase backscattering functions seems to be justified.

IV. DISCUSSION

The LiNbO_3 structure has been determined by x-ray and neutron diffraction.^{21–23} The structure is made up of irregular oxygen octahedra piled along the ferroelectric c axis and sharing faces. The centers of the octahedra are occupied by cations in the sequence Li^+ , Nb^{5+} , and a vacancy octahedron. Further, both Li^+ and Nb^{5+} are displaced (in opposite senses) along the c axis toward the neighbor vacancies. Detailed pictures of the structure are provided in the literature.^{6,9–11,21–23}

The radial distances of the neighboring atoms to the oxygen octahedron center are depicted in Figs. 8(a) and 8(b) for the Li and Nb positions, respectively. The distances are given as a function of the displacement δ from the point of the c axis equidistant from the upper and bottom faces of the oxygen octahedron (see Ref. 6). The displacement δ is considered positive in the positive direction of the ferroelectric c axis (i.e., in the direction lithium-niobium vacancy along the axis).

Li ions are not included in Fig. 8 because their contribution to the EXAFS signal should be minor due to the low backscattering amplitude of Li ($Z=3$). On the other hand, the vacancy site will not be considered because RBS experiments have demonstrated that the vacancy site is free of impurities in all the cases studied.^{9–11}

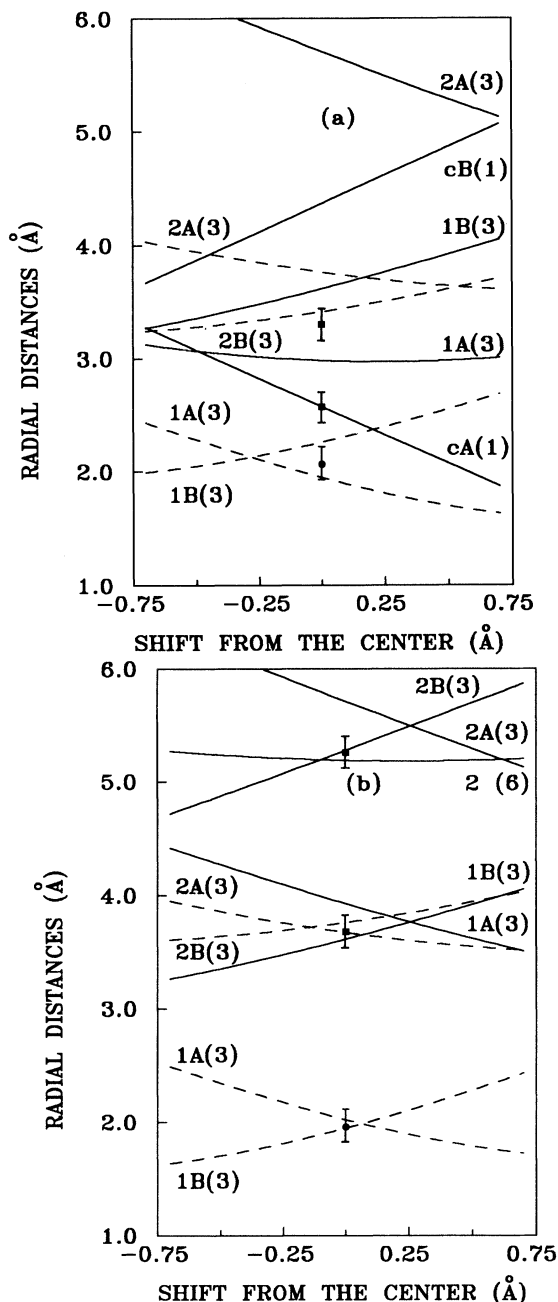


FIG. 8. Impurity-host ion radial distances calculated for oxygen (dashed line) and niobium (solid line) in the LiNbO_3 lattice as a function of the displacement δ from the center of the octahedron. The displacement is considered positive in the positive direction of the c axis (see Ref. 6). The center of the octahedron is considered as the point of the c axis equidistant from the two oxygen planes which form the first shell. The first digit in the notation stands for the order of the shell; ions along the c axis are denoted as c ; A and B denote ions belonging to the plane above (A) or below (B) the center; no letter means that the ions and center belong to the same plane; finally, the number in the brackets stands for the number of equivalent ions. Labels on the left side refer to oxygen distances and on the right to niobium distances. Experimental oxygen-related data are represented by circles and niobium-related ones by squares. (a) Li site. (b) Nb site.

A. Hf-doped samples

The distances reported in Table I for the Hf-O and Hf-Nb pairs have been compared with those expected in LiNbO_3 , shown in Fig. 8. The presence of a Hf-Nb peak at a distance of 2.57 Å suggests that the Hf peak lies in the Li octahedron. Moreover, the Hf-O shortest distance obtained by EXAFS better fits the average distance of the first-shell oxygens in the Li than in the Nb octahedron. Finally, the other distance corresponding to the Hf-Nb pair lies in between the distances of the six niobiums of the first shell lying above and below the center of the octahedron.

A plausible fit of the distances reported in Table I has been performed in Fig. 8(a). The fit is obtained if one assumes that impurity is close to the center of the oxygen octahedron. Within the experimental uncertainty, even a small shift of about -0.15 Å can be allowed.

The possibility that Hf is in the Nb site is much more unlikely: The average distance to the first oxygen shell is about one-tenth of an angstrom shorter, and according to Fig. 8(b), there are neither oxygen nor niobium neighbors between 2.1 and 3.5 Å; thus the Hf-Nb distances reported in Table I cannot be explained under this assumption of Hf being in the Nb octahedron.

B. Ta-doped samples

The treatment of the EXAFS spectrum shows the presence of a first coordination sphere at 1.96 Å that has been related to Ta-O pairs. This peak is consistent with the presence of the six oxygen atoms in the first shell. The distance of 1.96 Å seems to be too short when compared with the average distance of the first-shell oxygen atoms in the Li site [≈ 2.12 Å in Fig. 8(a)]. Additionally, no more peaks are found experimentally until the next niobium peak at 3.68 Å, and later a rather strong contribution of niobium atoms is present at 5.26 Å. These facts suggest that Ta is placed in the Nb octahedron.

We have plotted in Fig. 8(a) a plausible fit of our experimental distances with those expected in LiNbO_3 , assuming no displacement of the impurity from the center of the oxygen octahedron. With the 0.15 Å of error considered in the distances determined experimentally, the agreement is fairly good. In this case a positive shift of $+0.25$ Å is also possible.

Peak II of Fig. 6(a) does not seem to correspond to oxygen or niobium ions; however, the spectrum corresponding to LiTaO_3 also exhibits a similar II' peak, and indeed no oxygen or tantalum atoms exist in LiTaO_3 which can explain its presence. The only possibility (if this peak is not noise in both spectra) would be to relate them to Li ions.

V. CONCLUSIONS

In conclusion, we have found that Hf in LiNbO_3 lies in the Li site close to the center of the oxygen octahedron or maybe shifted in the negative sense of the c axis up to about 0.15 Å. This result agrees with the previous one obtained by RBS spectroscopy.¹¹

With regard to the Ta case, our results show that the impurity is close to the center of the niobium octahedron or possibly shifted along the positive direction of the c axis as much as 0.25 Å.

ACKNOWLEDGMENTS

The Spanish authors are indebted to LURE for the assistance and facilities provided to carry out this work as well as to the Ministry of Education of Spain for support-

ing the stand in LURE of Dr. C. Prieto with a grant. The authors are thankful to Professor F. Agulló-López for promoting EXAFS research on impurities in LiNbO_3 . This work has been partially supported by CICYT under Program No. MAT88-0431-C02-02.

-
- ¹M. N. Armenise, C. Canali, M. de Sario, and E. Zaroni, *Mater. Chem. Phys.* **9**, 267 (1983).
- ²E. Krätzig and O. F. Schirmer, in *Photorefractive Materials and their Applications I*, Vol. 61 of *Topics in Applied Physics*, edited by P. Günter and J. P. Huignard (Springer-Verlag, Berlin, 1988), Chap. 5.
- ³L. F. Johnson and A. A. Ballman, *J. Appl. Phys.* **40**, 297 (1969).
- ⁴D. A. Bryan, R. Gerson, and H. E. Tomaschke, *Appl. Phys. Lett.* **44**, 847 (1984).
- ⁵K. G. Belabaev, A. A. Kaminskii, and S. E. Sarkisov, *Phys. Status Solidi A* **28**, K17 (1975).
- ⁶C. Zaldo, F. Agulló-López, J. García, A. Marcelli, and S. Mobilio, *Solid State Commun.* **71**, 243 (1989).
- ⁷G. I. Malovichko and V. G. Grachev, *Fiz. Tverd. Tela (Leningrad)* **27**, 2789 (1985) [*Sov. Phys. Solid State* **27**, 1678 (1985)].
- ⁸G. Corradi, H. Söthe, J. M. Spaeth, and K. Polgár, *J. Phys. Condens. Matter* **2**, 6603 (1990).
- ⁹L. Rebouta, J. C. Soares, M. F. da Silva, J. A. Sanz-García, E. Diéguez, and F. Agulló-López, *Appl. Phys. Lett.* **55**, 120 (1989).
- ¹⁰L. Rebouta, J. C. Soares, M. F. da Silva, J. A. Sanz-García, E. Diéguez, and F. Agulló-López, *Nucl. Instrum. Methods Phys. Res. B* **45**, 495 (1990).
- ¹¹L. Rebouta, J. C. Soares, M. F. da Silva, J. A. Sanz-García, E. Diéguez, and F. Agulló-López, *Nucl. Instrum. Methods Phys. Res. B* **50**, 428 (1990).
- ¹²G. Charpak, R. Boucher, T. Bressani, J. Favier, and C. Zupancic, *Nucl. Instrum. Methods* **62**, 235 (1968).
- ¹³A. Gabriel, F. Dauvergne, and G. Rsenbaum, *Nucl. Instrum. Methods* **152**, 191 (1978).
- ¹⁴P. Fessler, M. Lemonnier, A. Gabriel, P. Bondot, B. Moraweck, and A. Renouprez (unpublished).
- ¹⁵B. K. Teo, *EXAFS: Basic Principles and Data Analysis. Inorganic Chemistry Concepts* (Springer-Verlag, Berlin, 1986), Vol. 9, Chap. 2.
- ¹⁶P. A. Lee and G. Beni, *Phys. Rev. B* **15**, 2862 (1977).
- ¹⁷A. G. Mckale, B. W. Veal, A. P. Paulikas, S. K. Chan, and G. S. Knapp, *J. Am. Chem. Soc.* **110**, 3763 (1988).
- ¹⁸S. C. Abrahams and P. Marsh, *Acta Crystallogr. B* **42**, 61 (1986).
- ¹⁹S. C. Abrahams and J. L. Bernstein, *J. Phys. Chem. Solids* **28**, 1685 (1967).
- ²⁰S. C. Abrahams, W. C. Hamilton, and A. Sequiera, *J. Phys. Chem. Solids* **28**, 1693 (1967).
- ²¹S. C. Abrahams, J. M. Reddy, and J. L. Bernstein, *J. Phys. Chem. Solids* **27**, 997 (1966).
- ²²Yoichi Shiozaki and Toshio Mitsui, *J. Phys. Chem. Solids* **24**, 1057 (1963).
- ²³S. C. Abrahams, W. C. Hamilton, and J. M. Reddy, *J. Phys. Chem. Solids* **27**, 1013 (1966).